

# Right handed neutrino production in dense and hot plasmas

Alejandro Ayala and Juan Carlos D'Olivo

*Instituto de Ciencias Nucleares*

*Universidad Nacional Autónoma de México*

*Apartado Postal 70-543, México D.F. 04510, México.*

Manuel Torres

*Instituto de Física*

*Universidad Nacional Autónoma de México*

*Apartado Postal 20-364, México D.F. 01000, México.*

## Abstract

For Dirac neutrinos with magnetic moment, we compute the production rate for right-handed neutrinos in a hot and dense QED plasma containing an initial population of left-handed neutrinos thermally distributed. The most important mechanisms for  $\nu_L$  depolarization, or production of right-handed neutrinos, are the  $\nu_L \rightarrow \nu_R$  chirality flip and the plasmon decay to  $\bar{\nu}_L + \nu_R$ . The rates for these processes are computed in terms of a resummed photon propagator which consistently incorporates the background effects to leading order. Applying the results to the cases of supernovae core collapse and the primordial nucleosynthesis in the early universe, we obtain upper limits on the neutrino magnetic moment.

PACS numbers: 11.10.Wx, 14.60.Lm, 95.30.Cq, 97.60.Bw

## I. INTRODUCTION

The properties of neutrinos have become the subject of an increasing research effort over the last years. Among these properties, the neutrino magnetic moment  $\mu_\nu$  has received attention in connection with various chirality flip processes that could have important consequences for the explanation of the solar neutrino problem [1,2], the dynamics of stellar collapse [3,4] and the evolution of the early universe [5]. A non-vanishing neutrino magnetic moment implies, for example, that left-handed neutrinos produced inside a supernova core during the collapse, could change their chirality becoming sterile with respect to the weak interaction. These sterile neutrinos would fly away from the star leaving essentially no energy to explain the observed luminosity of the supernova. The chirality flip could be caused by the interaction with an external magnetic field or by the scattering with charged fermions in the background, for instance  $\nu_L e^- \rightarrow \nu_R e^-$  and  $\nu_L p \rightarrow \nu_R p$ . Invoking this last mechanism and using the average parameters inferred from the supernova 1987A, Barbieri and Mohapatra [4] have derived a limit  $\mu_\nu < (0.2 - 0.8) \times 10^{-11} \mu_B$ , where  $\mu_B$  is the Bohr magneton.

It has also been pointed out that the constraints imposed by big-bang nucleosynthesis (BBN) do not allow the extra degree of freedom that a right-handed neutrino in equilibrium would introduce. In order to avoid that the chirality flip processes maintain a population of right-handed neutrinos in equilibrium during the evolution of the early universe, it is necessary that the average rate for these processes is less than the expansion rate of the universe at all times until the BBN epoch. Invoking this constraint, Elmfors *et. al.* [6] have derived a cosmological bound on the neutrino magnetic moment  $\mu_\nu < 6.2 \times 10^{-11} \mu_B$ .

Dispersion processes in a plasma could exhibit infrared divergences due to the long-range electromagnetic interactions. To prevent such divergences, the authors in Ref. [4] introduced an ad hoc thermal mass into the vacuum photon propagator. However, it is well known that at high temperatures or densities, a consistent formalism developed by Braaten and Pisarski [7,8] and that renders gauge independent results, requires the use of effective propagators and vertices that resum the leading-temperature corrections. The method has been successfully applied to the study of the damping rates and energy losses of particles propagating through hot plasmas [9–11]. In this paper we use this framework to study the neutrino chirality flip processes in a dense and hot plasma.

The most efficient process for conversion of left-handed to right-handed neutrinos happens through scattering off electrons with the exchange of effective space-like photons. In the resummation method of Braaten and Pisarski, these photons are described by the spectral function of the photon propagator that develops a non-vanishing contribution for space-like momenta and whose physical origin is Landau damping. We compute the production rate of  $\nu_R$ 's and the corresponding luminosity for such a process in a supernova. Our complete leading-order calculation is compared with the results obtained by means of an screening prescription used in a previous work [4]. Our result can be used to place an upper bound on the neutrino magnetic moment which is in the range  $\mu_\nu < (0.1 - 0.4) \times 10^{-11} \mu_B$  [12].

This work is organized as follows: In section II, we collect the ingredients that allow to compute the production rate of right-handed neutrinos from the imaginary part of the right-handed neutrino self-energy, in the real-time formulation of Thermal Field Theory (TFT), by means of a resummed photon propagator. In section III, we restrict the analysis to the

production of right-handed neutrinos from the chirality-flip process. We obtain approximate expressions for the production rate that permit us to explore its analytical behavior in the small and large right-handed neutrino energy regions. In section IV, we study the production of right-handed neutrinos through the plasmon decay process which we show to be subdominant as compared to the chirality flip process. In section V we use the average parameters inferred from the supernova 1987A to find an upper bound to the neutrino magnetic moment. In section VI, we also deduce an upper bound by imposing that the average production rate of right-handed neutrinos be at all times less than the Hubble rate up to the BBN epoch. This last result is shown to differ from that of Ref. [5]. We summarize our results in section VII and leave for the appendices some of the computations outlined throughout the rest of the work.

## II. FORMALISM

Consider a QED plasma in thermal equilibrium at a temperature  $T$  such that  $T, \tilde{\mu}_e \gg m_e$ , where  $m_e$  and  $\tilde{\mu}_e$  are the electron mass and chemical potential, respectively. The production rate  $\Gamma$  of right-handed neutrinos with total energy  $E$  and momentum  $\vec{p}$  can be conveniently expressed in terms of the  $\nu_R$  self-energy  $\Sigma$  as [13]

$$\Gamma(E) = \frac{n_F(E)}{2E} \text{Tr} [\not{p} R \text{Im} \Sigma] , \quad (1)$$

where  $L, R = \frac{1}{2}(1 \pm \gamma_5)$  and  $n_F$  is the Fermi-Dirac distribution for the right-handed neutrino. As shown below, in Eq. (2), the  $\nu_R$  thermal distribution cancels out from the final result. In what follows we consider  $E > 0$  corresponding to  $\nu_R$  production. The annihilation of  $\nu_R$  can be obtained from the case  $E < 0$ , however the initial  $\nu_R$  population is negligible and the corresponding rate can be ignored.

The resummation scheme is usually presented in the imaginary-time formalism. However, the expression for  $\text{Im}\Sigma$  can be directly computed following either the imaginary or the real-time formulations of TFT with identical results. In what follows we will work in the real-time formalism. As is well known, this formalism requires a doubling of the degrees of freedom and the propagators and self-energies adopt a  $2 \times 2$  matrix structure. In particular, the imaginary part of the retarded self-energy is related to the 1-2 component of the self-energy matrix through [14]

$$\text{Im} \Sigma(P) = \frac{\epsilon(E)}{2i n_F(E)} \Sigma_{12}(P) , \quad (2)$$

where  $\epsilon(E) = \theta(E) - \theta(-E)$ , with  $\theta$  the step function. As stated above the  $\nu_R$  thermal distribution cancels out when Eq. (2) is substituted in Eq. (1). We take  $\sigma = 0$  for the time path-parameter in the notation of Le Bellac [8] and Landsman and van Weert [14]. For simplicity we have selected the rest frame of the medium; however, the expressions can be rewritten in a covariant way replacing  $E$  by  $p \cdot u$ , where  $u_\mu$  is the velocity four-vector of the medium.

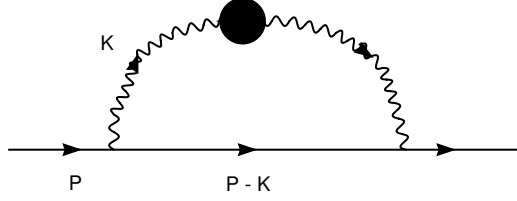


Fig. 1. Feynman diagram for the self energy  $\Sigma$  of the right-handed neutrino containing the effective photon propagator (resummed in the HTL approximation) denoted by a blob.

The one loop contribution to  $\Sigma_{12}$ , shown in Fig. 1, is given explicitly by

$$\Sigma_{12}(P) = -i\mu_\nu^2 \int \frac{d^4 K}{(2\pi)^4} K_\alpha \sigma^{\alpha\rho} S_{12}(\not{P} + \not{K}) L K_\beta \sigma^{\beta\lambda} {}^*D_{\rho\lambda}^{21}(K). \quad (3)$$

We will use capital letters to denote four-vectors:  $P^\mu = (E, \vec{p})$  for the incoming neutrino and  $K^\mu = (k_0, \vec{k})$  for the virtual photon, and  $p \equiv |\vec{p}|$ ,  $k \equiv |\vec{k}|$ . For the neutrino-photon vertex we take the magnetic dipole interaction  $\mu_\nu \sigma_{\alpha\beta} K^\beta$ . The neutrino effective electromagnetic vertices are of no concern to us here since they are induced by the weak interaction of the particles in the background and thus conserve chirality [15].

The intermediate  $\nu_L$  line can be taken as a bare fermion propagator because it gets dressed only through weak interactions with the particles in the medium. Hence, the  $S_{12}$  component for a massless fermion propagator is given by

$$S_{12}(Q) = 2\pi i Q \delta(Q^2) \epsilon(q_0) n_F(q_0), \quad (4)$$

where

$$n_F(q_0) = \frac{1}{e^{(q_0 - \tilde{\mu}_\nu)/T} + 1} \quad (5)$$

is the Fermi-Dirac distribution for the left-handed neutrino in the medium, with  $\tilde{\mu}_\nu$  being its chemical potential.

In Eq. (3), the integration region where the momentum  $k$  flowing through the photon line is soft (*i.e.* of order  $eT$ ) requires hard thermal loop (HTL) corrections to the photon propagator that contribute at leading order and must be resummed. The effective propagator is represented by the blob in Fig. 1, and is obtained by summing the geometric series of one-loop self-energy corrections proportional to  $e^2 T^2$ . As usual, we split the photon propagator into longitudinal and transverse parts

$${}^*D^{\mu\nu}(K) = {}^*D_L(K) P_L^{\mu\nu} + {}^*D_T(K) P_T^{\mu\nu}, \quad (6)$$

we drop the term proportional to the gauge parameter since it does not contribute to  $\Sigma$ , as can be easily checked. In the previous equation all  ${}^*D^{\mu\nu}$ ,  ${}^*D_T$  and  ${}^*D_L$  are  $2 \times 2$  matrices, while  $P_L^{\mu\nu}$  and  $P_T^{\mu\nu}$  are the longitudinal and transverse projectors, respectively,

$$\begin{aligned}
P_T^{00} &= P_T^{0i} = 0, & P_T^{ij} &= \delta^{ij} - \hat{k}^i \hat{k}^j, \\
P_L^{\mu\nu} &= -g^{\mu\nu} + \frac{K^\mu K^\nu}{K^2} - P_T^{\mu\nu}.
\end{aligned} \tag{7}$$

The effective photon propagator is obtained when the hard thermal loops in the photon self energy (first computed by Klimov [16] and Weldon [17]) are resummed. The complete matrix propagator is written as

$${}^*D_{L,T}(k) = \tilde{U} \begin{pmatrix} \frac{1}{k^2 - \Pi_{L,T} + i\epsilon} & 0 \\ 0 & \frac{-1}{k^2 - \Pi_{L,T}^* - i\epsilon} \end{pmatrix} \tilde{U}, \tag{8}$$

where  $\tilde{U}$  is the photon thermal matrix [14]. The polarization functions  $\Pi_L$  and  $\Pi_T$  are given by

$$\begin{aligned}
\Pi_L(K) &= -\frac{2m_\gamma^2 K^2}{k^2} \left[ 1 - \frac{k_0}{k} Q_0 \left( \frac{k_0}{k} \right) \right], \\
\Pi_T(K) &= \frac{m_\gamma^2 k_0}{k} \left[ \frac{k_0}{k} + \left( 1 - \left( \frac{k_0}{k} \right)^2 \right) Q_0 \left( \frac{k_0}{k} \right) \right],
\end{aligned} \tag{9}$$

$m_\gamma$  is the photon thermal mass, that in the limit  $T, \tilde{\mu}_e \gg m_e$  is given by

$$m_\gamma^2 = \frac{e^2}{6} \left( T^2 + \frac{3\tilde{\mu}_e^2}{\pi^2} \right). \tag{10}$$

The Legendre function  $Q_0(k_0/k)$  is defined in the complex  $k_0$  plane cut from  $-k$  to  $k$ ; it is real in the time-like region but it acquires an imaginary part for space-like  $K$

$$Q_0 \left( \frac{k_0}{k} \right) = \frac{1}{2} \ln \left| \frac{k_0 + k}{k_0 - k} \right| - i \frac{\pi}{2} \theta(k^2 - k_0^2). \tag{11}$$

The solution of the equations  $K^2 - Re\Pi_L = 0$  and  $K^2 - Re\Pi_T = 0$  represent the propagation of longitudinal photons, or plasmons, and transverse photons, respectively. These solutions in the time-like region are well known, in general they are obtained numerically. However it is possible to obtain approximate analytical results for small and large values of  $k$ . In the small momentum limit  $k \ll m_\gamma$  the dispersion relations reduce to

$$\begin{aligned}
\omega_T^2 &= \omega_p^2 + \frac{6}{5} k^2, \\
\omega_L^2 &= \omega_p^2 + \frac{3}{5} k^2,
\end{aligned} \tag{12}$$

where the plasma frequency is defined as  $\omega_p = \sqrt{\frac{2}{3}} m_\gamma$ . In the large momentum limit  $k \gg m_\gamma$  the behavior of the dispersion relations is approximated by

$$\begin{aligned}
\omega_T^2 &= m_\gamma^2 + k^2, \\
\omega_L &= k + 2k \exp \left( -\frac{k^2}{m_\gamma^2} \right).
\end{aligned} \tag{13}$$

In a relativistic plasma the photon dispersion relation for the longitudinal mode  $K^2 - Re\Pi_L = 0$  has also a solution in the space-like region [18]. Then the Čerenkov radiation of a plasmon is, in principle, kinematically allowed. The numerical solution of the longitudinal dispersion for  $\omega < k$  is shown in Fig. 2. We observe that the solution is close to the light cone. Using this fact and the first of Eqs. (9), it is a simple task to derive the following approximate solution

$$\omega_L = k - 2k \frac{1}{1 + \exp\left(\frac{k^2 + 2m_\gamma^2}{m_\gamma^2}\right)}, \quad (14)$$

that, as shown in Fig. 2, agrees very well with the numerical solution. However, this mode develops a large imaginary part, which implies that the Landau damping mechanism acts to preclude its propagation. In this situation the correct method to include the complete contribution of both the space-like and time-like degrees of freedom requires the use of the spectral representation as given below in Eq. (16). The effect of the space-like mode is not very distinctive, except for the low energy spectrum of the  $\nu_R$  production via the spin flip reaction  $\nu_L \rightarrow \nu_R$  (see next section).

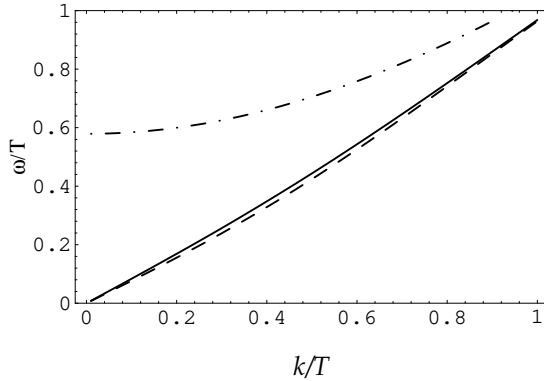


*Fig. 2. Dispersion relations for the longitudinal modes. The upper branch (dotted - dashed line) is the usual time-like solution. The lower branch is the space-like mode. The numerical solution (solid line) is compared with the approximate analytical result (dashed line).*

From Eqs. (8) and (9) we can get the component  ${}^*D^{21}$  of the photon propagator. In order to obtain the complete result, we notice that for time-like momenta the  $\Pi_L$  and  $\Pi_T$  functions are real, however for space-like momenta both functions acquire an imaginary part as seen from Eqs. 9 and 11. The final result can be written as

$${}^*D_{L,T}^{21} = 2\pi i [1 + f(k_0)] \rho_{L,T}(k_0, k), \quad (15)$$

where  $f(k_0) = (e^{k_0/T} - 1)^{-1}$  is the Bose-Einstein distribution and the functions  $\rho_{L,T}(k_0, k)$  are given by

$$\rho_i(k_0, k) = Z_i(k) [\delta(k_0 - \omega_i(k)) + \delta(k_0 + \omega_i(k))] + \beta_i(k_0, k) \theta(k_0^2 - k^2), \quad (16)$$

for  $i = L, T$ . The residue  $Z_L(k)$  for the longitudinal excitations is given by

$$Z_L(k) = \frac{\omega_L(k)}{k^2 + 2m_\gamma^2 - \omega_L^2(k)}, \quad (17)$$

and the cut function  $\beta_L(k_0, k)$

$$\beta_L(k_0, k) = \left( \frac{x}{x^2 - 1} \right) \frac{m_\gamma^2}{\left[ k^2 + 2m_\gamma^2 \left( 1 - \frac{x}{2} \ln \left| \frac{x+1}{x-1} \right| \right) \right]^2 + \left[ \pi m_\gamma^2 x \right]^2}, \quad (18)$$

where we have defined  $x \equiv k_0/k$ . For the transverse mode, the residue and cut functions are given by

$$Z_T(k) = \frac{\omega_T(k) (\omega_T^2(k) - k^2)}{2m_\gamma^2 \omega_T^2(k) - (\omega_T^2(k) - k^2)^2}, \quad (19)$$

$$\beta_T(k_0, k) = \frac{(1/2)m_\gamma^2 x (1 - x^2)}{\left[ k^2(1 - x^2) + m_\gamma^2 \left( x^2 + \frac{x}{2}(1 - x^2) \ln \left| \frac{x+1}{x-1} \right| \right) \right]^2 + \left[ \frac{\pi}{2} m_\gamma^2 x (1 - x^2) \right]^2}. \quad (20)$$

The functions  $\rho_{L,T}(\omega, k)$  are referred to as the photon spectral densities. It is a straightforward exercise to verify that these coincide with the spectral densities computed in the imaginary-time formalism after the analytical continuation to real time is performed. The spectral densities  $\rho_{L,T}(\omega, k)$  contain the discontinuities of the photon propagator across the real- $\omega$  axis. Their support depends on the magnitude of the ratio between  $\omega$  and  $k$ . For  $|\omega/k| > 1$ ,  $\rho_{L,T}(\omega, k)$  have support on the points  $\pm\omega_{L,T}(k)$ , i.e., the time-like quasiparticle poles. In the space-like region the support of  $\rho_{L,T}(\omega, k)$  lies on the whole interval  $-k < \omega < k$ , with the contribution arising from the branch cut of  $Q_0$ . Hence, the spectral density is the sum of pole and cut terms.

To proceed with the calculation of Eqs. (1) and (3) we need the following quantities

$$\begin{aligned} C_T(E, K) &\equiv K_\alpha K_\beta P_{T\mu\nu} \text{Tr} \left[ \sigma^{\alpha\mu} (\not{P} + \not{K}) L \sigma^{\beta\nu} \not{P} R \right] = k^2 (x^2 - 1)^2 \left[ (2E + \omega)^2 - k^2 \right], \\ C_L(E, K) &\equiv K_\alpha K_\beta P_{L\mu\nu} \text{Tr} \left[ \sigma^{\alpha\mu} (\not{P} + \not{K}) L \sigma^{\beta\nu} \not{P} R \right] = -k^2 (x^2 - 1)^2 (2E + \omega)^2. \end{aligned} \quad (21)$$

The production rate of right-handed neutrinos in Eq. (1) can be computed after the substitution of the expressions for the fermion, Eq. (2), and photon, Eq. (15), propagators into Eq. (3). Using also the spectral representations, Eq. (16), our result is

$$\begin{aligned} \Gamma(E) &= \frac{\mu_\nu^2 \pi^2}{E} \int \frac{d^4 k}{(2\pi)^4} \epsilon(E + k_0) \epsilon(k_0) (1 + f(k_0)) n_F(E + k_0) \\ &\quad [C_L(E, K) \rho_L(k_0, k) + C_T(E, K) \rho_T(k_0, k)]. \end{aligned} \quad (22)$$

As we have already mentioned we shall consider  $E > 0$  corresponding to the production of  $\nu_R$ . However, depending on the signs of  $E + \omega$  and  $\omega$  the  $\nu_R$  production rate can be divided into the chirality flip process  $\nu_L \rightarrow \nu_R$  mediated by a virtual photon and the plasmon decay process  $\gamma \rightarrow \bar{\nu}_L \nu_R$ . We shall analyze these two processes separately in the following sections.

### III. THE $\nu_L \rightarrow \nu_R$ CHIRALITY FLIP

The contribution to the  $\nu_L \rightarrow \nu_R$  chirality flip process is obtained from the general expression in Eq. (22) if we set  $E + \omega > 0$  as corresponds to the case of an incident  $\nu_L$ . The angular integration over the direction of  $\vec{k}$  is readily performed. Using the condition  $|\cos \Theta| \leq 1$ , where  $\Theta$  is the angle between the momenta of the incoming neutrino and the virtual photon, we obtain two kinematical restrictions, namely,  $|\omega| \leq k$  and  $(k - \omega) \leq 2E$ . The first condition implies that for the chirality flip  $\nu_L \rightarrow \nu_R$  process the kinematically allowed region is restricted to  $|\omega| < k$  and consequently the only contribution from the photon spectral density in Eq. (16) arises from the cuts. The rate of production of right-handed neutrinos from the  $\nu_L \rightarrow \nu_R$  flip can be computed after the substitution of the expressions for the fermion, Eq. (2), and photon, Eq. (15), propagators into Eq. (3), the result is

$$\Gamma(E) = \frac{\mu_\nu^2}{16\pi E^2} \int_0^\infty k dk \int_{-k}^k d\omega \theta(2E + \omega - k) (1 + f(\omega)) n_F(E + \omega) [C_L(E, K) \beta_L(\omega, k) + C_T(E, K) \beta_T(\omega, k)] , \quad (23)$$

where we set  $k_0 = \omega$ . Both, longitudinal and transverse photons, contribute to this rate. Notice that using the restriction  $(k - \omega) \leq 2E$ , the integrand in the previous equation can be proved to be positive definite. The rate  $\Gamma$  can be written as the sum of two contributions  $\Gamma = \Gamma_e + \Gamma_a$ , that correspond to the production of  $\nu_R$  through the emission or absorption of a virtual photon.  $\Gamma_e$  comes from the interval  $0 \leq \omega < k$ , whereas  $\Gamma_a$  corresponds to the interval  $-k < \omega \leq 0$ , as can be checked by means of the identity  $1 + f(\omega) + f(-\omega) = 0$  and the substitution  $\omega \rightarrow -\omega$  in this second interval.

The results for the longitudinal and transverse contributions to  $\Gamma(E)$  as a function of  $E$  are shown in Fig. 3, for a selection of values characteristic of a supernova core (see section V). The solution for the chirality flip production rate requires in general numerical integration. However, the physical interpretation of the results is made clearer with approximate analytical solutions that can be derived both in the small and large energy limits.

Let us first consider the region of small neutrino energy ( $E \ll T, \tilde{\mu}_\nu$ ). From Fig. 3, we observe that the longitudinal contribution shows a pronounced peak at energies below 5 MeV. The result is somewhat unexpected because in the study of similar processes, the effect of infrared logarithmic singularities shows up in the transverse contributions. For example, in the calculation of the lifetime of a fermion quasiparticles in a  $QED$  plasma at high temperature the soft photon contribution leads to an infrared divergence in the transverse component alone due to the vanishing of the magnetic mass. The problem was solved with the use of a non-perturbative method based on a generalization of the Bloch-Nordsieck approximation [19]. In the present case, there are enough powers of  $k$  coming from the vertex factors in Eq. (3) to render the transverse contribution finite in the infrared. We will show this explicitly in appendix A. On the other hand the longitudinal photon is known to be screened by the Debye mass in the  $\omega = 0, k \rightarrow 0$  limit, yet our results lead to a pronounced peak at small  $E$ . As we shall see, this effect arises because the longitudinal spectral density, Eq. (18), has a logarithmic divergence at the light cone. A qualitative way to understand this behavior stems from the observation that there also exists a space-like branch for the longitudinal mode [18], though with a large imaginary part that precludes propagation of the



mode. This branch lies very close to the light-cone. Could we ignore the large damping that the mode experiences, the situation would correspond to a process in which a left-handed neutrino changes its chirality becoming a right-handed neutrino through the emission or absorption of a Čerenkov photon. As we cannot ignore damping, the contribution shows up as that from a resonance that peaks for small right-handed neutrino energies, that is, for the region where the difference  $k - \omega \gtrsim 0$  is small.

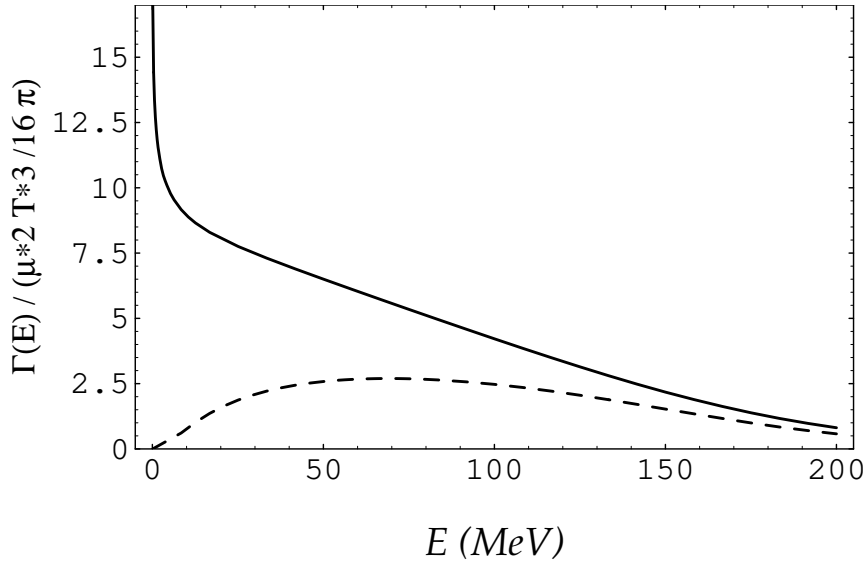


Fig. 3. The Longitudinal (solid line) and transverse contributions (dashed line) to the production rate  $\Gamma(E)$  for right-handed neutrinos via the spin flip transition  $\nu_L \rightarrow \nu_R$ .

Let us consider the limit  $E \rightarrow 0$ , then the virtual photon is forced to be near the light cone ( $\omega \lesssim k$ ). The integration in Eq. (23) is restricted to the kinematical region  $\omega \leq k \leq 2E + \omega$ , hence in the limit  $E \rightarrow 0$  we may set  $k = E + \omega$  everywhere in the  $k$ -integration. Keeping only the leading term in  $E$ , the cut contributions to the spectral densities can be replaced by the approximate expressions

$$\begin{aligned} \beta_T &= \frac{E}{\omega m_\gamma^2}, \\ \beta_L &= -\frac{\omega}{2E m_\gamma^2 [\ln(E/T)]^2}, \end{aligned} \quad (24)$$

where in the last expression we have simplified the approximation by replacing  $\omega$  by its mean value  $T$ . We notice that the dependence on the longitudinal spectral function that originates the strong rise at small  $E$  comes from the fact that near the light cone  $\beta_L$  behaves as  $1/[\ln(k - \omega)]^2$ . Using the previous results and the identity

$$[1 + f(\omega)] [n_F(E + \omega)] = n_F(E) [f(\omega) + n_F(E + \omega)], \quad (25)$$

the resulting integrals can be evaluated analytically. Separating  $\Gamma(E)$  into its transverse and longitudinal parts, we obtain for the transverse contribution in the limit  $E \rightarrow 0$

$$\Gamma_T(E) \approx \frac{\mu_\nu^2 E^3 T^2}{\pi m_\gamma^2} n_F(0) \left[ Li_2 \left( -e^{\tilde{\mu}_\nu/T} \right) - \frac{\pi^2}{6} \right], \quad (26)$$

where  $Li_n(z) = PolyLog[n, z]$  is the PolyLog function [20]. For the longitudinal part the result reads

$$\Gamma_L(E) \approx \frac{6\mu_\nu^2 T^5}{\pi m_\gamma^2} \frac{n_F(0)}{[\ln(E/T)]^2} \left[ Li_5 \left( -e^{\tilde{\mu}_\nu/T} \right) - \zeta(5) \right], \quad (27)$$

where  $\zeta(z)$  is the Riemann zeta function. Both contributions vanish at  $E = 0$ , however the longitudinal part shows a steep rise for small  $E$  that originates the peak observed in Fig. 3. The maximum for the longitudinal spectrum can also be estimated and it is attained for a very small value of the energy

$$E \approx T \exp \left( -\frac{T^2}{m_\gamma^2} \right). \quad (28)$$

The previous results show that the  $\nu_L \rightarrow \nu_R$  chirality flip reaction produces a huge number of small energy right-handed neutrinos. While this effect looks remarkable, the phenomena that it can give rise to are probably unobservable because at very low neutrino energies, experimental discrimination between the charged current interactions of low energy  $\nu_R$  and  $\nu_L$  would be fairly difficult. We also notice that in this limit, the reaction rate  $\Gamma(E)$  depends nonlinearly on the coupling constant  $e$ .

We now turn our attention to the limit in which the neutrino energies are larger or of order  $T$ ,  $\tilde{\mu}_\nu$ . As we shall see, a very good analytical approximation can be obtained in this case. The method extracts explicitly the leading logarithmic screening terms that arise from the use of the full resummed propagator. Following Braaten and Yuan [11] we introduce and intermediate cut-off  $q^*$  such that  $m_\gamma \ll q^* \ll T, \tilde{\mu}_\nu$ . In the region of hard momentum transfer  $k > q^*$  the tree-level approximation is used for the virtual photon,  $q^*$  acting as an infrared regulator. In the soft region  $k < q^*$ , the effective resummed propagator is used. Adding the hard and soft contributions, the dependence on the arbitrary scale  $q^*$  cancels.

Let us first outline the calculation of the soft-momentum transfer contribution to  $\Gamma(E)$ . In this region, hard thermal loop corrections to the photon propagator are not suppressed by powers of  $e$ , hence the resummed photon propagator must be used. Restricting our attention to the momentum region  $k < q^*$  we can set  $1 + f(\omega) \approx T/\omega$  and for the functions in Eq. (21) we make the approximations

$$C_T(E, K) \approx -C_L(E, K) \approx \frac{4K^4 E^2}{k^2} \quad (29)$$

inserting the results into Eq. (23), this last reduces to

$$\Gamma_{soft}(E) = \frac{\mu_\nu^2 T n_F(E)}{4\pi} \int_0^{q^*} k^3 dk \int_{-k}^k \frac{d\omega}{\omega} \left( 1 - \frac{w^2}{k^2} \right)^2 [\beta_T(\omega, k) - \beta_L(\omega, k)]. \quad (30)$$

The integral over  $\omega$  can be evaluated by using the sum rules derived from the analytical properties of the effective propagators [21]

$$\int_{-k}^k d\omega \omega^{2n-1} \left(1 - \frac{\omega^2}{k^2}\right) \beta_L = -2 \left(1 - \frac{\omega_L^2}{k^2}\right) \omega_L^{2n-1} Z_L + k^{2n-2} \left[ \frac{2m_\gamma^2}{2m_\gamma^2 + k^2}, \frac{2m_\gamma^2}{3k^2} \right] \quad (31)$$

for  $n = 0, 1,$

$$\int_{-k}^k d\omega \omega^{2n-1} \beta_T = -2\omega_T^{2n-1} Z_T + k^{2n-2} \left[ 1, 1, \frac{2m_\gamma^2 + 3k^2}{3k^2} \right] \quad (32)$$

for  $n = 0, 1, 2.$

The logarithmic dependence on  $q^*$  can be extracted analytically, the result is

$$\Gamma_{soft}(E) = \frac{\mu_\nu^2 m_\gamma^2 T}{2\pi} n_F(E) \left( \ln \left[ \frac{q^*}{\sqrt{2}m_\gamma} \right] + \int_0^\infty dk \left[ \frac{(\omega_L^2 - k^2)^2}{m_\gamma^2 k \omega_L} Z_L - \frac{(\omega_T^2 - k^2)^2}{m_\gamma^2 k \omega_T} Z_T \right] \right), \quad (33)$$

where we used the fact that  $m_\gamma \ll q^*$  and have extended the limit of integration to  $\infty$  since we are just interested in the leading contribution. The remaining integral inside the brackets is a dimensionless quantity and can be computed numerically with the result  $-0.14$ .

We now turn to the hard-momentum transfer contribution to  $\Gamma(E)$ . In this region the tree-level photon propagator must be used. Following Le Bellac [8] we notice that tree-level results can be recovered from the full calculation by simply neglecting  $m_\gamma^2$  in the denominators of Eqs. (18) and (20). Hence, the approximated spectral densities yield

$$-\beta_L \approx 2\beta_T \approx \frac{m_\gamma^2 \omega / k^3}{k^2 - \omega^2}. \quad (34)$$

It is convenient to further decompose the hard region ( $k > q^*$ ) into a (I) low ( $\omega < q^*$ ) and (II) high ( $\omega > q^*$ ) frequency regions. In the low frequency region we can still use the approximations  $1 + f(\omega) \approx T/\omega$  and Eq. (29). The remaining integrations are readily performed. Recalling that  $q^* \ll E$ , the result is

$$\Gamma_{hard}^I(E) = \frac{2\mu_\nu^2 m_\gamma^2 T}{3\pi} n_F(E). \quad (35)$$

In the high frequency region it is not obvious that we can neglect  $\omega$  and  $k$  as compared to  $E$ , in particular the approximation in Eq. (29) may not be accurate. However for  $E \sim T$ ,  $\tilde{\mu}_\nu$  the integrals are dominated by small  $\omega$  and  $k$ , hence neglecting  $\omega, k$  as compared with  $E$  yields the the leading order contribution in  $T/E$ . The approximation can be improved for large  $E$ , by computing the next order term, the second order corrections are given in appendix B. Thus to leading order we can set  $\omega, k \rightarrow 0$  as compared with  $E$  wherever possible, except for the Bose and Fermi distributions that provide the cutoff for the integrals and must be taken exact. Using the identity in Eq. (25) we obtain

$$\Gamma_{hard}^{II}(E) = \frac{\mu_\nu^2 m_\gamma^2 T}{2\pi} n_F(E) \left[ \ln \left( \frac{T}{q^*} \right) + \ln \left( 1 + e^{(E - \tilde{\mu}_\nu)/T} \right) + \frac{1}{2} \ln \left( \frac{1 - e^{-E/T}}{1 + e^{-\tilde{\mu}_\nu/T}} \right) + \frac{E - \tilde{\mu}}{T} \right]. \quad (36)$$

The complete rate for the production of right handed neutrinos to leading order in  $e$  is the sum of Eqs. (30), (33) and (35). The result is

$$\Gamma(E) = \frac{\mu_\nu^2 m_\gamma^2 T}{2\pi} n_F(E) \left[ C + \ln \left( \frac{T}{\sqrt{2} m_\gamma} \right) + \frac{3(E - \tilde{\mu}_\nu)}{4T} \right. \\ \left. + \frac{1}{2} \ln \left( \frac{\cosh^2 \left( \frac{E - \tilde{\mu}_\nu}{2T} \right) \sinh \left( \frac{E}{2T} \right)}{\cosh \left( \frac{\tilde{\mu}_\nu}{2T} \right)} \right) \right], \quad (37)$$

where  $C = 1.88$ . Note that the dependence on the arbitrary intermediate scale  $q^*$  cancels out between the soft contribution in Eq. (30) and the hard contribution in Eq. (35). In Fig. 4, we display the comparison of this analytical approximation with the result of the numerical integration of the exact result in Eq. (23). We notice that for energies in the region  $E \gg T, \tilde{\mu}_\nu$  the analytical result gives an excellent approximation to the exact result. As mentioned before the result can be improved by computing the next order correction in  $T/E$ . Fig. 4 also shows the result of the second order contribution calculated in appendix B.

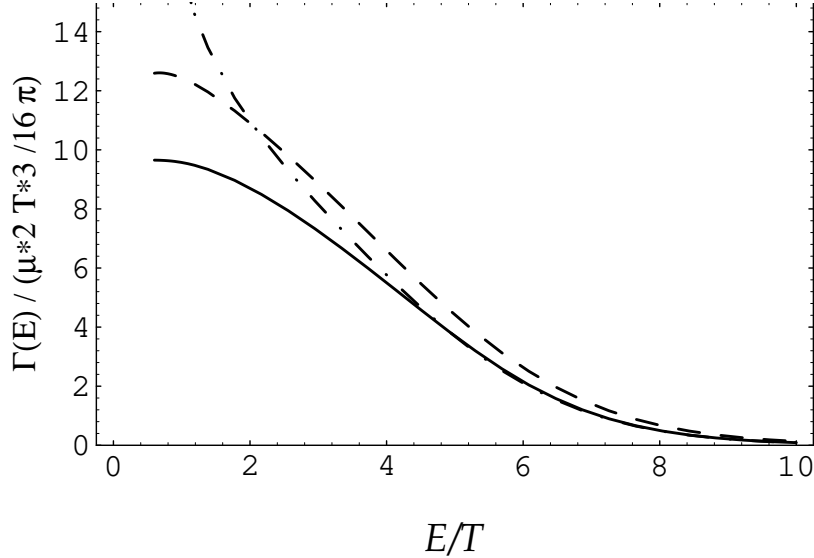


Fig. 4. The production rate  $\Gamma(E)$  for right-handed neutrinos via the spin flip transition  $\nu_L \rightarrow \nu_R$ . The exact (numerical) result in the solid line is compared with the approximate result (dashed line) to leading order in  $T/E$  and the approximate result (dotted-dashed line) to second order in  $T/E$ .

The energy carried by the produced right-handed neutrinos or  $\nu_R$  emissivity  $q$  can be obtained from  $\Gamma(E)$  according to the relation

$$q = \int \frac{d^3 p}{(2\pi)^3} E \Gamma(E). \quad (38)$$

The  $\nu_R$  energy spectrum ( $\propto E^3 \Gamma(E)$ ) as a function of  $E$  is shown in Fig. 5, where the exact numerical result, shown as solid line, is compared with the approximate analytical results.

We observe an excellent agreement between the exact and the second order approximate solution.

Finally, we quote that in the degenerate limit  $T \rightarrow 0$ ,  $\Gamma(E)$  reduces to a very simple expression

$$\Gamma(E) = \frac{\mu_\nu^2 m_\gamma^2}{4\pi} (\tilde{\mu}_\nu - E) \theta(\tilde{\mu}_\nu - E), \quad (39)$$

which is similar to the one obtained in Ref. [22] for the damping rate of a fermion in a QED dense relativistic plasma at zero temperature.

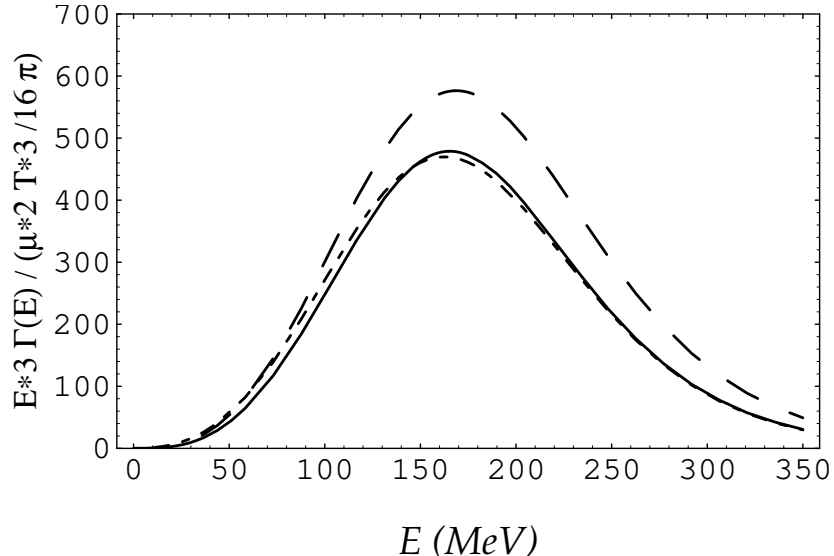


Fig. 5 The energy spectrum  $\sim E^3 \Gamma(E)$  for right-handed neutrinos produced by the spin flip transition  $\nu_L \rightarrow \nu_R$ . The exact (numerical) result in the solid line is compared with the approximate result (dashed line) to leading order in  $T/E$  and the approximate result (dotted line) to second order in  $T/E$ .

#### IV. PLASMON TO $\bar{\nu}_L \nu_R$ DECAY

We now consider the contribution to the  $\nu_R$  production rate arising from the plasmon decay process  $\gamma \rightarrow \bar{\nu}_L \nu_R$ . The rate is obtained from the general expression in Eq. (22) by setting  $E + k_0 < 0$  as corresponds to a negative energy  $\nu_L$  or an outgoing  $\bar{\nu}_L$ . The angular integration over the direction of  $\vec{k}$  leads now to the following kinematically restrictions

$$\begin{aligned} \omega &\equiv -k_0 > 0 \\ \omega^- &\leq E \leq \omega^+. \end{aligned} \quad (40)$$

where  $\omega^\pm = (\omega \pm k)/2$ . These restrictions imply that for the plasmon decay process, the kinematically allowed region corresponds to the time-like region  $|\omega| > k$  and thus the contribution from the photon spectral density in Eq. (16) arises solely from the poles. Using the identities

$$1 + f(-\omega) = -f(\omega)$$

$$\tilde{n}_F(-E') = 1 - \frac{1}{e^{(E' + \tilde{\mu}_\nu)/T} + 1} = 1 - \tilde{n}_F(E'), \quad (41)$$

where  $\tilde{n}_F$  refers to the thermal distribution of  $\bar{\nu}_L$ , we can obtain the  $\nu_R$  production rate from the plasmon decay process. Substituting the expressions for the fermion and photon propagators, Eqs. (2) and (15), into Eq. (3) we obtain

$$\Gamma(E) = \frac{\mu_\nu^2}{16\pi E^2} \sum_{i=L,T} \int_0^\infty k dk \theta(\omega^+ - E) \theta(E - \omega^-) f(\omega_i(k)) [1 - \tilde{n}_F(\omega_i(k) - E)]$$

$$C_i(E, -\omega_i(k)) Z_i(k), \quad (42)$$

where the sum is carried over the longitudinal and transverse modes. The  $\nu_R$  emissivity can now be computed using Eq. (38). In general, the  $E$  and  $k$  integrations have to be computed numerically, however, in many applications we can consider that the  $\bar{\nu}_L$  neutrinos are absent from the medium. Then, the Pauli blocking factor can be neglected, and the integration over the  $\nu_R$  energy can be readily performed with the result

$$q = \frac{\mu_\nu^2}{96\pi^3} \int_0^\infty k^2 dk \left[ \frac{1}{2} \omega_L(k) (\omega_L^2(k) - k^2)^2 f(\omega_L(k)) Z_L(k) \right.$$

$$\left. + \omega_T(k) (\omega_T^2(k) - k^2)^2 f(\omega_T(k)) Z_T(k) \right]. \quad (43)$$

The remaining integral still requires numerical computation. However, analytic expressions can be obtained in the limit cases  $m_\gamma \ll T$  and  $m_\gamma \gg T$ . In order to discuss these limits, it is convenient to decompose the emissivity  $q$  into its longitudinal and transverse parts  $q_L$  and  $q_T$ .

The limit  $m_\gamma \ll T$  requires ultrarelativistic temperatures and, according to Eq. (10), an electron density bound by the condition  $e\tilde{\mu}_e \ll \sqrt{2}\pi T$ . In this limit, the integral for the transverse emissivity in Eq. (43) is dominated by  $k$  on the order of  $T$ . Thus, we can use the large  $k$  limit of the dispersion relation in Eq. (13) and the resulting integral can be evaluated analytically with the result

$$q_T = \frac{\mu_\nu^2 \zeta(3)}{96\pi^3} m_\gamma^4 T^3, \quad (44)$$

where  $\zeta(z)$  is the Riemann zeta function.

For the longitudinal emissivity in the same limit  $m_\gamma \ll T$ , the contributions for large  $k$  can be neglected. The reason is that the substitution of the asymptotic expansion, Eq. (13), in the factor  $(\omega_L(k)^2 - k^2)^2$  produces a Gaussian cutoff in the integrals. Thus, the integral is dominated by  $k$  on the order of  $m_\gamma$  or smaller. The Bose distribution can be approximated by  $f(\omega_L) \sim T/\omega_L$ . The integral then involves only the scale  $m_\gamma$  and can be evaluated numerically

$$q_L = 0.28 \frac{\mu_\nu^2}{96\pi^3} m_\gamma^6 T. \quad (45)$$

We notice that in this limit the longitudinal emissivity is negligible as compared to the transverse emissivity, since it is suppressed by a factor  $(m_\gamma/T)^2$ .

The limit  $T \ll m_\gamma$  is obtained for an ultrarelativistic electron density and low temperatures according to the relation  $e\tilde{\mu}_e \gg \sqrt{2}\pi T$ . In this limit the integrals in both the longitudinal and transverse cases are dominated by momenta small compared to  $m_\gamma$ . We can set  $k \rightarrow 0$  wherever possible except that, according to the asymptotic expansion in Eq. (12), the Bose distribution is approximated by  $f \rightarrow \exp[-(\omega_p + \lambda k^2/\omega_p)/T]$  with  $\lambda = 3/5, 3/10$  for the transverse and longitudinal modes respectively. The resulting integrals can be evaluated analytically with the results

$$\begin{aligned} q_T &= \frac{\mu_\nu^2}{768\pi^3} \left(\frac{125\pi}{27}\right)^{1/2} \omega_p^{11/2} T^{3/2} e^{-\omega_p/T}, \\ q_L &= \frac{\mu_\nu^2}{768\pi^3} \left(\frac{250\pi}{27}\right)^{1/2} \omega_p^{11/2} T^{3/2} e^{-\omega_p/T}. \end{aligned} \quad (46)$$

## V. THE $\nu_R$ EMISSION IN A SUPERNOVA

As a first application of our results we consider the emission of right-handed neutrinos immediately after a supernova core collapse. The large mean free path of the right handed neutrinos compared to the core radius implies that the  $\nu_R$ 's would freely fly away from the supernova. Therefore, the core luminosity for  $\nu_R$  emission can be simply computed as

$$Q_{\nu_R} = V q, \quad (47)$$

where  $V$  is the plasma volume and  $q$  is the  $\nu_R$  emissivity computed from Eq. (38). To make a numerical estimate, we shall adopt a simplified picture of the inner core, corresponding to the the average parameters of SN1987A [23,24]. Consequently, we take a constant density  $\rho \approx 8 \times 10^{14} \text{ g/cm}^3$ , a volume  $V \approx 8 \times 10^{18} \text{ cm}^3$ , an electron to baryon ratio  $Y_e \simeq Y_p \simeq 0.3$ , and temperatures in the range  $T = 30 \sim 60 \text{ MeV}$ . This corresponds to a degenerate electron gas with a chemical potential  $\tilde{\mu}_e$  ranging from 307 to 280 MeV. For the left-handed neutrino we take  $\tilde{\mu}_\nu \approx 160 \text{ MeV}$ . Using this values in Eqs. (23) and (47), we obtain by numerical integration

$$Q_{\nu_R} = \left(\frac{\mu_\nu}{\mu_B}\right)^2 (0.7 - 4.3) \times 10^{76} \text{ ergs/sec}, \quad (48)$$

for  $T$  ranging from 30 to 60 MeV. The main contribution to this result arises from the  $\nu_L \rightarrow \nu_R$  flip process, whereas the contribution from the  $\gamma \rightarrow \bar{\nu}_L \nu_R$  decay is smaller by two orders of magnitude. This result is in agreement with the observation first made by Fukugita and Yazaki [25] who noticed that for cosmological and astrophysical scenarios the plasmon decay process is subdominant as compared to the chirality flip process. Moreover, an estimate of the  $\nu_R$  luminosity derived from the approximate solutions discussed in section III are surprisingly accurate, they differ from the result in Eq. (48) by less than 2%.

Assuming that the emission of  $\nu_R$ 's lasts approximately for 1 sec., the luminosity bound is  $Q_{\nu_R} \leq 10^{53} \text{ ergs/sec.}$  which places the upper limit on the neutrino magnetic moment

$$\mu_\nu < (0.1 - 0.4) \times 10^{-11} \mu_B. \quad (49)$$

This upper bound slightly improves the result previously obtained by Barbieri and Mohapatra [4]. As mentioned before, these authors consider the helicity flip scattering  $\nu_L e \rightarrow \nu_R e$  to order  $e^4$  introducing the Debye mass in the photon propagator as an infrared regulator.

A word of caution should be mentioned in relation to the result in Eq. (49). It has been pointed out by Voloshin [26] that the  $\nu_R$ 's produced by the magnetic moment interaction could undergo resonant conversion back into  $\nu_L$ 's through spin rotation in the magnetic field of the supernova core, with the subsequent trapping of the  $\nu_L$ 's by the external layers. If this is the case, then the bound in Eq. (49) becomes meaningless. However, the core density is rather high and the matter effect might dominate over the  $\mu_\nu B$  term, suppressing the flip back of  $\nu_R$  to  $\nu_L$  [23].

Recently, another mechanism for the neutrino chirality flip has been proposed, which occurs via the Čerenkov emission or absorption of plasmons in the supernova core [27]. Since the photon dispersion relation in a relativistic plasma shows a space-like branch for the longitudinal mode, the Čerenkov radiation of the plasmon is, in principle, kinematically allowed [18]. However, this mode develops a large imaginary part, which implies that the Landau damping mechanism acts to preclude its propagation as we have discussed. Consequently, we think that no better than the quoted limit in Eq. (49) can be derived by this type of neutrino chirality flip processes in a supernova core.

## VI. EARLY UNIVERSE

As a second application of our results, we now consider the production of right-handed neutrinos during the evolution of the early universe. If the rate of production of these neutrinos is able to maintain them in thermal contact with the rest of the particles in the plasma, then they will contribute to the effective number of degrees of freedom until their final decoupling. This could in principle affect primordial nucleosynthesis. In order to prevent right-handed neutrinos from being in thermal equilibrium, we need to require that their average production rate be less than the Hubble rate at all times until the neutrino freeze-out epoch. During the radiation dominated era, the Hubble rate was

$$H = \frac{T^2}{m_{Plank}} \left( \frac{4\pi^3}{45} g_* \right)^{1/2}, \quad (50)$$

with  $g_* \simeq 10.75$  the effective number of degrees of freedom at the nucleosynthesis epoch. On the other hand, the average right-handed neutrino production rate can be obtained from Eq. (23) (neglecting the contribution from the plasmon decay process) by averaging with an equilibrium distribution

$$n_\nu(E) = \frac{1}{\exp(E/T) + 1}, \quad (51)$$

appropriate for the early universe where the chemical potentials should be negligible. Therefore, the condition to avoid populating the right-handed neutrino component becomes

$$\langle \Gamma \rangle = 5.78 \times 10^{-4} T^3 \mu_\nu^2 < \frac{T^2}{m_{Plank}} \left( \frac{4\pi^3}{45} g_* \right)^{1/2}, \quad (52)$$



where for nucleosynthesis,  $100 \text{ MeV} > T > 1 \text{ MeV}$ . The most stringent bound on  $\mu_\nu$  is obtained for the highest possible temperature and thus we take  $T = 100 \text{ MeV}$  which yields

$$\mu_\nu < 2.9 \times 10^{-10} \mu_B. \quad (53)$$

This result has to be compared to that from Ref. [6] where the use of a *full one-loop* approximation to the photon polarization functions is used, instead of Eqs. (9). This choice leads to an upper bound one order of magnitude smaller than the above. One should notice however that when a plasma is such that the largest energy scale available is set by the temperature (or density), as in the present scenario, it is necessary to select the leading temperature (density) contributions out of perturbative calculations and sum these up into effective vertices and propagators in order to extract from them meaningful quantities. In this manner, one can ensure that the leading perturbative corrections are effectively taken into account [7]. Therefore, we conclude that the bound on the neutrino magnetic moment set by nucleosynthesis constraints is not nearly as stringent as that set by the analysis of a supernova core collapse.

## VII. CONCLUSIONS

In conclusion, we have shown that the scattering processes mediated by effective plasma photons allows for the efficient conversion of  $\nu_L$  into  $\nu_R$ . In this work, plasma effects are consistently taken into account by means of the resummation method of Braaten and Pisarski within the real-time formulation of TFT. For soft values of the energy, the production rate of  $\nu_R$  differs significantly from that obtained by a constant Debye mass screening prescription. However, corrections to the integrated luminosity are small and for this reason, our upper bound on the neutrino magnetic moment does not differ significantly from the one obtained by Barbieri and Mohapatra [4]. Knowledge of an accurate expression for the  $\nu_R$  production rate, as given in Eq. (23), could be of importance in a detailed analysis of supernova processes. We also obtain another constraint on  $\mu_\nu$  by considering the possible effect of  $\nu_R$  production in the early universe. The upper bound imposed by the analysis of SN1987A is two orders of magnitude smaller than the one obtained from the nucleosynthesis constraint.

## VIII. APPENDIX A

In this appendix, we want to explicitly show that the transverse photon contribution,  $\Gamma_T(E)$ , to the right-handed neutrino production rate,  $\Gamma(E)$ , is free from infrared divergences. To this end, we refer back to Eqs. (20) and (23) that give the explicit expression for  $\Gamma_T(E)$ . Let us write  $x = \omega/k$  thus, when  $x \rightarrow 0$ , we can write

$$1 + f(kx) \rightarrow \frac{T}{kx}, \quad (54)$$

where  $f(z)$  is the photon statistical distribution. Notice that in this limit,  $\beta_T(k, x)[1 + f(kx)]$  remains finite, unless we also take  $k \rightarrow 0$ . Let us write

$$\beta_T(k, x) = \frac{1}{k^2(1-x^2)} \tilde{\beta}_T(k, x), \quad (55)$$

with the definition

$$\tilde{\beta}_T(k, x) \equiv \frac{k^2 m_\gamma^2 x (1-x^2)^2 / 2}{\left[ k^2(1-x^2) + m_\gamma^2 \left( x^2 + \frac{x}{2}(1-x^2) \ln \left( \frac{1+x}{1-x} \right) \right) \right]^2 + \left[ \pi m_\gamma^2 x \frac{(1-x^2)}{2} \right]^2}. \quad (56)$$

Notice that for  $x \ll 1$ ,

$$\frac{\tilde{\beta}_T(k, x)}{x} \rightarrow \frac{m_\gamma^2}{2} \frac{k^2}{k^4 + (\pi m_\gamma^2 x / 2)^2}. \quad (57)$$

Therefore, in the limit  $k \rightarrow 0$ ,

$$\frac{\tilde{\beta}_T(k, x)}{x} \rightarrow \delta(x). \quad (58)$$

In this manner, we can write the contribution to  $\Gamma_T(E)$  from the soft ( $k \rightarrow 0, \omega \rightarrow 0$ ) region as

$$\begin{aligned} \Gamma_T^{soft}(E) &\approx \frac{\mu_\nu^2 T}{16\pi E^2} n_F(E) \int_0^{m_\gamma} dk k \theta(2E - k) [(2E)^2 - k^2] \\ &= \frac{\mu_\nu^2 T}{16\pi E^2} n_F(E) \begin{cases} m_\gamma^2 (2E^2 - m_\gamma^2 / 4), & 2E \geq m_\gamma \\ 4E^4, & 2E < m_\gamma \end{cases}, \end{aligned} \quad (59)$$

where in the integration we have set as the upper limit the soft scale  $m_\gamma$ . This choice is somewhat arbitrary but it does not matter as long as for the hard contribution to  $\Gamma_T(E)$  we integrate  $k$  from  $m_\gamma$ . Eq. (59) is thus explicitly infrared finite.

## IX. APPENDIX B

The second order correction in  $(T/E)$  to  $\Gamma(E)$  for the quirkality flip  $\nu_L \rightarrow \nu_R$  reaction can also be calculated analytically. As discussed in section III, the leading order term is obtained by setting  $\omega, k \rightarrow 0$  as compared with  $E$  wherever possible, except for the Bose and Fermi distributions. In the soft-momentum region, the condition  $\omega, k \ll E$  is valid everywhere, and consequently there are no  $T/E$  corrections to the result in Eq. (33).

The hard-momentum region ( $k > q^*$ ) was decomposed into a (I) low ( $\omega < q^*$ ) and (II) high frequency ( $\omega > q^*$ ) regions. In the low frequency region we have  $\omega \ll E$  and only  $k/E$  corrections have to be computed. It is a simply exercise to show that the only corrections are of order  $(T/E)^2$ , hence the result in Eq. (35) is not modified in the next order. Finally, in the high frequency region we compute corrections of order  $k/E$  and  $\omega/E$  to the result in Eq. (36). In particular, instead of Eq. (29), we approximate the functions in Eq. (21) by

$$C_T(E, K) \approx -C_L(E, K) \approx \frac{4K^4}{k^2} (E^2 + E\omega). \quad (60)$$

The correction to the result in Eq. (36) is given in terms of PolyLog functions as

$$\Gamma(E) = \frac{\mu_\nu^2 m_\gamma^2 T}{2\pi} n_F(E) \left[ \left( \frac{T}{8E} \right) \left( -\pi^2 + 7Li_2 \left( e^{-E/T} \right) + 7Li_2 \left( -e^{\tilde{\mu}_\nu/T} \right) - 8Li_2 \left( -e^{(\tilde{\mu}_\nu - E)/T} \right) \right) \right. \\ \left. + 7 \left( \frac{E}{T} \right) \ln \left( \frac{1 + e^{\tilde{\mu}_\nu/T}}{1 - e^{-E/T}} \right) - \frac{7}{2} \left( \frac{E}{T} \right)^2 \right]. \quad (61)$$

This corrections improve the approximate analytical solution given in Eq. (37) when compared with the exact result in Eq. (23) for energies  $E \gtrsim T, \tilde{\mu}_\nu$ , as shown in Figs. 4 and 5.

## ACKNOWLEDGMENTS

This work was supported in part by Universidad Nacional Autónoma de México under Grants DGAPA-IN117198 and DGAPA-IN10389, and by CONACyT-México under Grants 3097 p-E and I27212-E.

## REFERENCES

- [1] A. Cisneros, *Astrophys. Space Sci.* **10**, 87 (1970).
- [2] M. B. Voloshin and M. I. Vysotsky, *Sov. J. Nucl. Phys.* **44**, 845 (1986); M. B. Voloshin, M. I. Vysotsky and L. B. Okun, *Sov. Phys. JETP* **64**, 446 (1986).
- [3] S. Nussinov and Y. Raphaeli, *Phys. Rev. D* **36**, 2278 (1987) ; I. Goldman, Y. Aharonov, G. Alexander and S. Nussinov, *Phys. Rev. Lett.* **60**, 1789 (1988); J.M. Lattimer and J. Cooperstein, *Phys. Rev. Lett.* **61**, 23 (1988); D. Nötzold, *Phys. Rev. D* **38**, 1658 (1988).
- [4] R. Barbieri and R. N. Mohapatra, *Phys. Rev. Lett.* **61**, 27 (1988).
- [5] B.D. Fields, K. Kainulainen and K.A. Olive, *Astropart. Phys.* **6** 169 (1997).
- [6] P. Elmfors, K. Enqvist, G. Raffelt and G. Sigl, *Nucl. Phys. B***503**, 3 (1997).
- [7] E. Braaten and R. D. Pisarski, *Nucl. Phys. B***337**, 569 (1990).
- [8] M. Le Bellac, *Thermal Field Theory*. Cambridge University Press (1996).
- [9] E. Braaten and R. D. Pisarski, *Phys. Rev. D* **42**, 2156 (1990).
- [10] E. Braaten and M. H. Thoma, *Phys. Rev. D* **44**, 1298 (1991).
- [11] E. Braaten and T. C. Yuan, *Phys. Rev. Lett.* **66**, 2183 (1991).
- [12] A. Ayala, J.C. D’Olivo and M. Torres, *Phys. Rev. D* **59**, 111901 (1999).
- [13] H. A. Weldon, *Phys. Rev. D* **26**, 1394 (1982).
- [14] N. P. Landsman and Ch. G. van Weert, *Phys. Rep.* **145**, 141 (1987).
- [15] J.C. D’Olivo, J.F. Nieves and P.B. Pal, *Phys. Rev. D* **40**, 3679 (1989).
- [16] V. V. Klimov, *Sov. J. Nucl. Phys.* **33**, 934 (1981).
- [17] H. A. Weldon, *Phys. Rev. D* **26**, 2789 (1982).
- [18] J.C. D’Olivo and J.F. Nieves, *Phys. Rev. D* **57**, 3116 (1997).
- [19] J. P. Blaizot and E. Iancu, *Phys. Rev. Lett.* **76**, 3080 (1996).
- [20] M. H. Lee, *J. Math. Phys. (N.Y.)* **36**, 1217 (1995).
- [21] R. D. Pisarski, *Phys. Rev. D* **47**, 5589 (1993).
- [22] M. Le Bellac and C. Manuel, *Phys. Rev. D* **55**, 3215 (1997).
- [23] R. N. Mohapatra and P. B. Pal, *Massive neutrinos in physics and astrophysics*. World Scientific Vol. 60, (1997).
- [24] A. Burrows, *Annu. Rev. Nucl. Part. Sci.* **40**, 181 (1990); S. E. Woosley and T. A. Weaver, *Annu. Rev. Astron. Astrophys.* **24**, 205 (1986).
- [25] M. Fukugita and S. Yazaki, *Phys. Rev. D* **36**, 3817 (1987).
- [26] M. B. Voloshin, *Phys. Lett. B***209**, 360 (1988).
- [27] S. Mohanty and S. Sahu, *Neutrino helicity flip by Čerenkov emission and absorption of plasmons in supernova*, hep-ph/9710404.